AiMT

Advances in Military Technology
Vol. 13, No. 2 (**2018**), pp. 173-183
ISSN 1802-2308, eISSN 2533-4123
DOI 10.3849/aimt.01227

Dynamic Lift and Vortex Breakdown during an Unsteady Flow over a Pitching Airfoil

A. Svoboda* and D. Rozehnal

University of Defence in Brno, Czech Republic

The manuscript was received on 22 December 2017 and was accepted after revision for publication on 17 May 2018.

Abstract:

Computational fluid dynamics techniques are used to give a detailed insight into unsteady phenomena taking place in the vicinity of a pitching airfoil. The vortex formation and breakdown are analyzed using the time history of pressure distribution, vorticity and injected massless particle trajectories. Different cases of flows are modeled to determine the effect of reduced frequency on unsteady lift. Finally, a comparison of lift coefficients for steady and unsteady cases is provided.

Keywords:

unsteady aerodynamics, dynamic lift, vortex, pitching, airfoil, NACA 0012, CFD

1. Introduction

Unsteady flows represent an interesting and current area of aerodynamics with plenty of applications spanning multiple fields. It can be argued that every real world aerodynamic application is to a certain extent affected by unsteady phenomena. Highly maneuverable combat aircraft capable of flying at high angles of attack and able to reach these high values of α very quickly are one of the most interesting examples. Helicopter rotor blades, cascade turbine discs, naval vessel propellers, and the effects of atmospheric phenomena on high-rising buildings represent several other applications in the technical field, while pulsing blood in the vessels and the foundations of insect flight are two examples from the area of biology. In supersonic aerodynamics, the interaction between shock waves and the boundary layer is of particular significance. This paper aims to analyze the unsteady phenomena related to a pitching NACA 0012 airfoil, using the methods of computational fluid dynamics.

A flow can be characterized as unsteady only if its quantities are time-dependent when referenced to the Eulerian frame, in which the flow field is a function of position in space and time. Unlike in the case of rigid body mechanics, a great part of fluid

* *Corresponding author: Department of Air Force and Aircraft Technology, University of Defence in Brno, Kounicova 65, 662 10 Brno, Czech Republic, E-mail: Ales.Svoboda@army.cz*

dynamics problems is classified as steady with all their quantities being time-independent. The unsteady viscous flow field of study covers two main sets of problems – the influence of external dynamic disturbances on the viscous flow, and the problems related to self-generated and self-sustained unsteady flow fields. This paper is focused on the first group of problems, specifically on the effect of external transient or periodic disturbances on the fluid flow.

2. Foundations of Unsteady Flows

A flow field is characterized by four variables: velocity, pressure, density and temperature. These quantities are determined by a system of four equations: the equation of state, and the laws of conservation of mass, inertia (Newton's second law of motion applied to the control volume) and energy. It can be assumed that flow properties reach their undisturbed values at infinity, as we are dealing with external aerodynamics. Also, no suction or blowing of the boundary layer is assumed to take place along the object's wall. The flow in our case is considered incompressible, hence the density and viscosity are constant. Thus, the system of the three laws of conservation can be simplified into the following form:

$$\frac{\partial u_i}{\partial x_i} = 0\,, \tag{1}$$

$$\rho\left(\frac{\partial u_i}{\partial t} + u_j \frac{\partial u_i}{\partial x_j}\right) = \rho g_i - \frac{\partial p}{\partial x_i} + \mu \frac{\partial^2 u_i}{\partial x_j \partial x_j}\,, \tag{2}$$

$$\rho c_v \left(\frac{\partial T}{\partial t} + u_j \frac{\partial T}{\partial x_j}\right) = k \frac{\partial^2 T}{\partial x_j \partial x_j} + \Phi\,. \tag{3}$$

As a result, the velocity field becomes independent on the heat field. By dividing the Eq. (2), the Navier-Stokes equation, by density, we get the following:

$$\left(\frac{\partial}{\partial t} + u_j \frac{\partial}{\partial x_j} - \upsilon \frac{\partial^2}{\partial x_j \partial x_j}\right) u_i = -\frac{\partial w}{\partial x_i} + g_i\,. \tag{4}$$

The quantity u is velocity vector, p is pressure, T is temperature, c_v is specific heat at constant volume, k is heat transfer coefficient, g is gravitational acceleration, t and x are independent time and space variables, ρ is density, μ is dynamic viscosity, Φ is a dissipation function, υ is kinematic viscosity, w is specific thermodynamic work. The velocity field is then obtained by solving the Navier-Stokes equation. The other quantities of our interest (e.g. pressure) can then be calculated.

When the airfoil pitches rapidly, the viscous flow in the boundary layer is lagging the motion of the airfoil. Due to a slow increase in the thickness of the boundary layer, the flow separation does not occur even at angles of attack higher than the steady critical value. When the pitching motion is initiated, a bubble is soon formed on the suction side of the airfoil. When the angle of attack is increased beyond its stationary critical value, the negative pressure gradient bubble grows and ultimately bursts, creating a vortex, which then moves along the airfoil towards the trailing edge. It is important to note that this differentiates the dynamic separation from the steady case, in which the separation of the flow originates at the trailing edge of the airfoil and moves towards the leading edge. When the airfoil is dynamically stalled, the lift curve

forms a hysteresis loop, and the flow does not reattach until the angle of attack is significantly decreased, usually well below its steady critical value.

The unsteady flow can be characterized by several parameters, of which the reduced frequency is arguably the most important one. It is defined as follows:

$$k = \frac{\omega c}{2U}. \tag{5}$$

The reduced frequency k is a measure of flow unsteadiness: $k = 0$ represents a steady flow, whereas $0 < k \leq 0.05$ is considered quasi-steady, while $k > 0.05$ marks an unsteady case. The quantity ω is angular frequency, c is airfoil chord length, U is velocity of the free flow.

3. CFD Modeling

Computational fluid dynamics techniques were used to model the unsteady flow around a pitching airfoil.

3.1. Scope of Modeling

The flow over a NACA 0012 airfoil conducting a simple harmonic pitching motion about the quarter-chord point within the angle of attack range of 5 to 25° and 0 to 30° was studied for different Reynolds numbers of the undisturbed flow and for different reduced frequencies. Overall, nine different cases of flows were examined.

The Reynolds numbers ranged from 9.5×10^4 to 5.5×10^6. The reduced frequencies were between 0.01 and 0.94.

3.2. Method Used

The ANSYS 16.2 software platform with its Fluent module was used for the simulation. A C-grid mesh with approximately 20 000 nodes and near-wall adjustment was utilized to capture the flow in all boundary sublayers. Different mathematical models for a two-dimensional flow field simulation were utilized, dominantly the SST k-ω model. Also, a three-dimensional DDES model was used to simulate the vortex structures in the flow field. In this case, a two-dimensional airfoil had to be replaced with a three-dimensional wing section of a 1.9812 m (6.5 ft) span and a constant chord of 1.2192 m (4 ft). The computational domain of the flow field was side-walled to prevent the phenomena related to a finite span from occurring.

3.3. Model Validation

A subset of the studied cases of unsteady flows was in the α-range of 5 to 25° with $Re = 2.5 \times 10^6$ and $k = 0.05$, 0.15, and 0.25, to allow for a validation of the CFD model against experimental data obtained at a NASA wind tunnel by [1].

4. Results

Using the data obtained by CFD modeling, the process of vortex formation and breakdown can be visualized and described. Furthermore, the steady and unsteady lift coefficient values can be compared, and the effect of major flow and motion parameters can be assessed.

4.1. Unsteady Vortex Formation and Breakdown Visualization

Five different phases of vortex formation, breakdown and flow reattachment were observed during the unsteady flow over a pitching NACA 0012, as depicted in Figs 1 – 10. First, a bubble is formed on the suction side of the airfoil close to the leading edge, with a minor bubble at about three quarters of the chord (Fig. 1). A vortex is then formed at the position of the bubble in the vicinity of the leading edge (Fig. 2). The vortex then shifts towards the trailing edge (Fig. 3), separates itself from the airfoil and breaks down, while another smaller vortex is formed at the trailing edge (Figs 4 and 5). This subsequent vortex also separates (Fig. 6) and breaks down, while a third vortex is formed at approximately one third of the chord (Fig. 7). The third small vortex rapidly separates (Fig. 8) and breaks down (Fig. 9). The flow becomes reattached after the airfoil pitches back down below approximately 10° of angle of attack (Fig. 10).

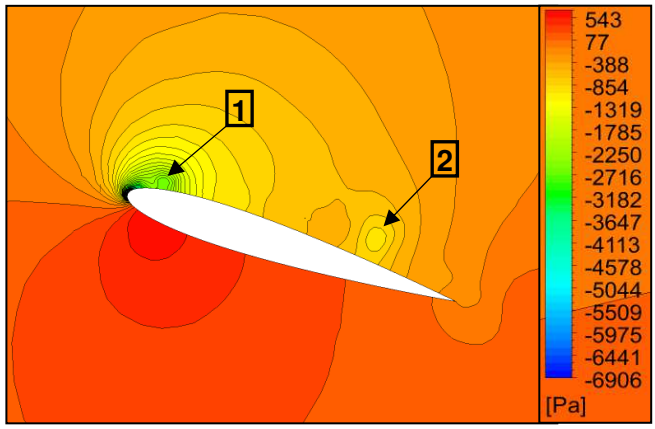

Fig. 1 Negative pressure gradient bubble formation (pressure distribution, DDES, side-walled NACA 0012 wing section, half-span, α = 5 to 25°, $Re = 2.5 \times 10^6$, k = 0.15)

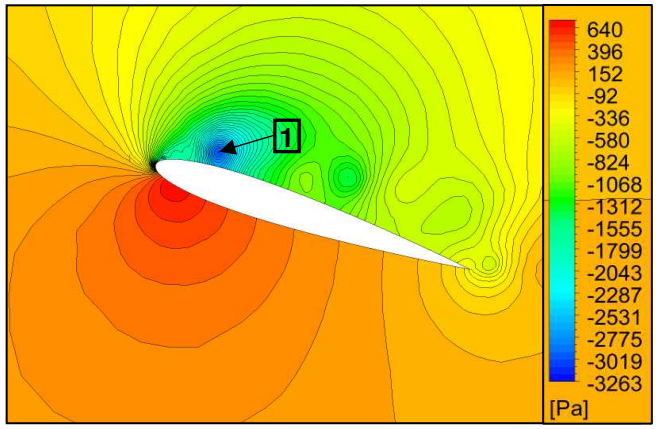

Fig. 2 Vortex formation (pressure distribution, DDES, side-walled NACA 0012 wingsection, half-span, α = 5 to 25°, $Re = 2.5 \times 10^6$, k = 0.15)

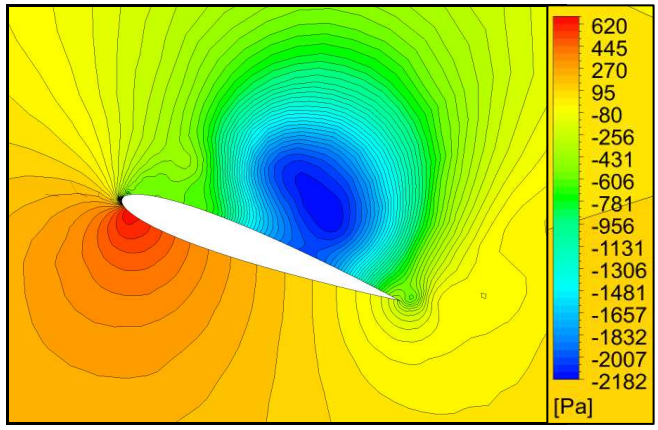

Fig. 3 Vortex shifting towards the trailing edge (pressure distribution, DDES, side-walled NACA 0012 wing section, half-span, α = 5 to 25°, $Re = 2.5 \times 10^6$, k = 0.15)

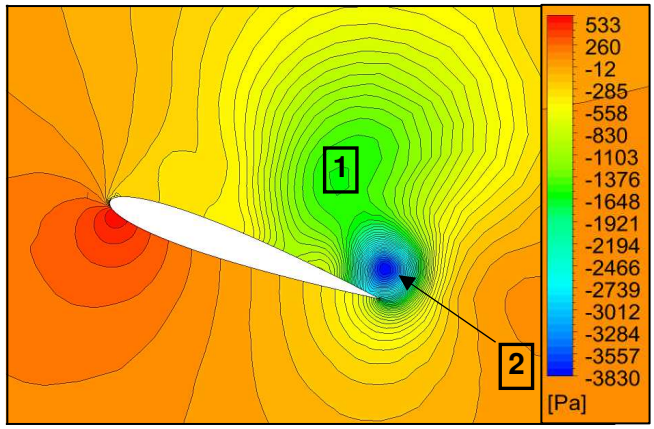

Fig. 4 Main vortex breakdown and consequent smaller vortex formation (pressure distribution, DDES, side-walled NACA 0012 wing section, half-span, α = 5 to 25°, $Re = 2.5 \times 10^6$, k = 0.15)

4.2. Unsteady and Steady Lift Comparison

The overall set of nine cases of flows that were studied was comprised of two subsets of cases of flows. One with the angle of attack range of 5 to 25°, the other with α ranging from 0 to 30°.

In the first subset, the maximum steady value of the coefficient of lift was exceeded by 28 to 33 %, proportionally to the reduced frequency. In the second subset (α ranging from 0 to 30°), the maximum stationary lift coefficient was exceeded by 37 to 75 % (and by only 8 % for the quasi-steady case of k = 0.01). The greatest lift increase of 75 % occurred at k = 0.47 (the reduced frequencies ranged from 0.01 to 0.94). For very high k, the maximum lift increase over the steady case was a bit lower, but still very significant (58 %).

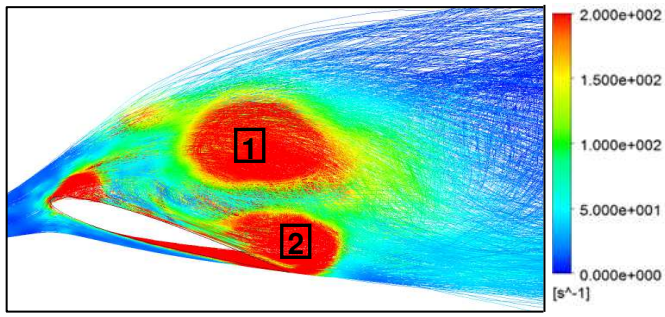

Fig. 5 Main vortex breakdown and consequent smaller vortex formation (massless particles trajectories colored by vorticity, DDES, side-walled NACA 0012 wing section, half-span, α = 5 to 25°, $Re = 2.5 \times 10^6$, k = 0.15)

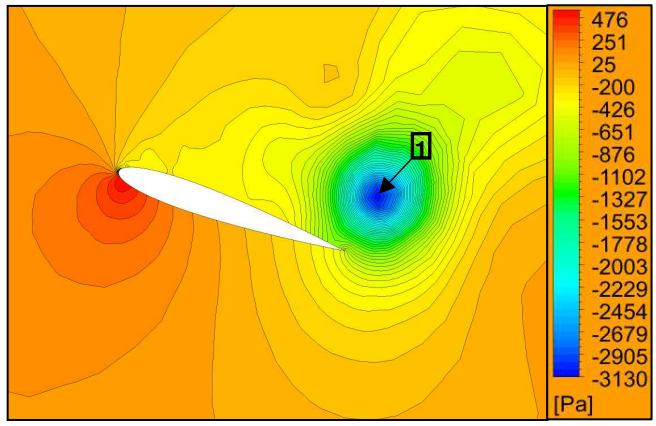

Fig. 6 Subsequent smaller vortex separation (pressure distribution, DDES, side-walled NACA 0012 wing section, half-span, α = 5 to 25°, $Re = 2.5 \times 10^6$, k = 0.15)

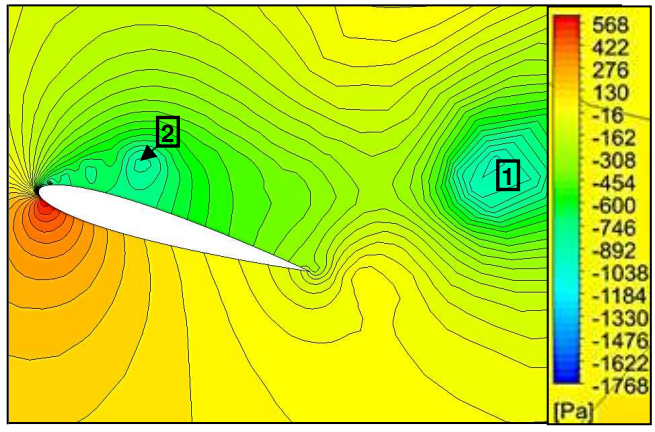

Fig. 7 Subsequent smaller vortex breakdown and a third small vortex formation (pressure distribution, DDES, side-walled NACA 0012 wing section, half-span, α = 5 to 25°, $Re = 2.5 \times 10^6$, k = 0.15)

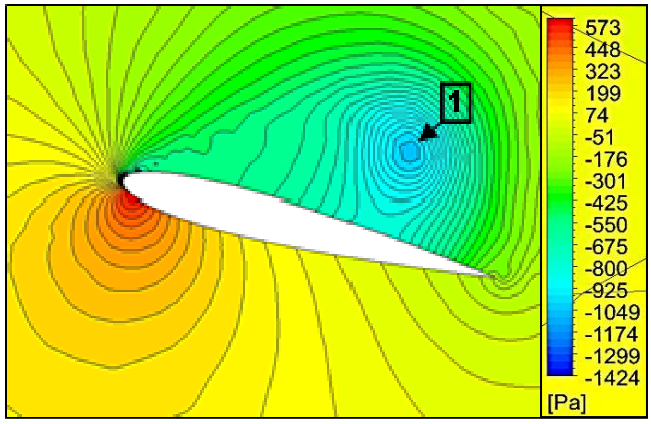

Fig. 8 Rapid separation of the third small vortex (pressure distribution, DDES, side-walled NACA 0012 wing section, half-span, α = 5 to 25°, $Re = 2.5 \times 10^6$, k = 0.15)

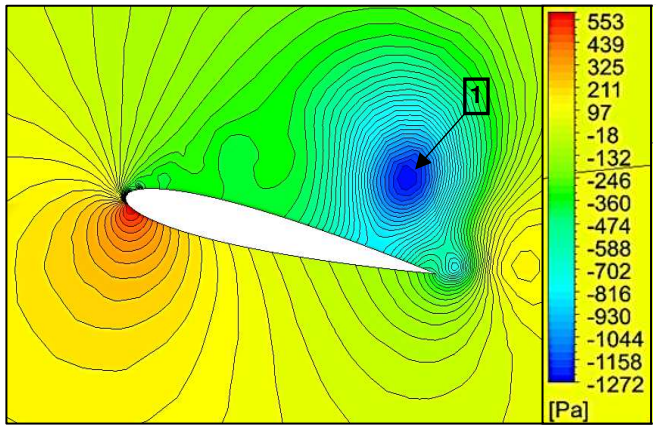

Fig. 9 Third small vortex breakdown (pressure distribution, DDES, side-walled NACA 0012 wing section, half-span, α = 5 to 25°, $Re = 2.5 \times 10^6$, k = 0.15)

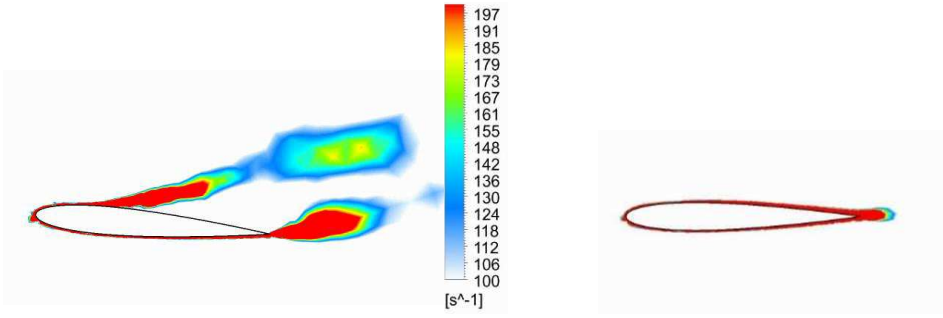

Fig. 10 Flow reattachment at α = 10° and 5° (vorticity, DDES, side-walled NACA 0012 wing section, half-span, α = 5 to 25°, $Re = 2.5 \times 10^6$, k = 0.15)

When compared to the steady case, the angle of attack corresponding to the maximum lift coefficient was also surpassed. In the first subset (5 to 25° of angle of attack), the unsteady values were 18 to 37 % greater than the steady ones. Again, the higher values were reached at higher reduced frequencies, specifically for $k = 0.15$ and $k = 0.25$. In the second subset (0 to 30° of angle of attack), the stationary $\alpha_{CL\max}$ values were surpassed even more – by 51 to 92 %. The steady $\alpha_{CL\max}$ was exceeded even in the quasi-steady case ($k = 0.01$) – by 39 %. The greatest $\alpha_{CL\max}$ increase of 92 % was observed for $k = 0.47$. For very high k, the increase over the steady case was smaller, but still significant (52 %).

When comparing individual periods of the harmonic pitching motion, it was observed that for different reduced frequencies the maximum lift was achieved in different periods of the motion. However, the differences between the first, the second and the third period were negligible (in the order of 0.0001 to 0.001 for the maximum C_L values). On the other hand, the maximum values of C_L were reached at the same angles of attack for all three periods. The only exception was a high reduced frequency motion ($k = 0.94$), where the maximum coefficient of lift differed for the first, the second and third period (2.31, 2.06 and 2.05, respectively). The corresponding angles of attack were also different (25.0°, 26.8°, and 28.2°, respectively).

4.3. The Effect of Reynolds Number and Reduced Frequency on Unsteady Lift

The lift curve obtained by CFD modeling of the unsteady flow over a pitching NACA 0012 for $\alpha = 5$ to 25°, $Re = 2.5 \times 10^6$, and $k = 0.15$ was compared with numerical data from [2], which covered a pitching motion with the same parameters except for the Reynolds number, which was 1.0×10^6. It was observed that the difference in Reynolds number did not significantly affect the lift curve. In both cases, the rk-ε mathematical model was used.

Conversely, when a comparison of four cases of flow of different reduced frequencies was made ($k = 0.01$, 0.12, 0.47 and 0.94), the obtained lift curves differed very significantly. In all cases, the angle of attack range was 0 to 30° and the rk-ε mathematical model was used. The lowest reduced frequency of these four cases of flow represents a quasi-steady case, while the remaining three cases of flow are fully unsteady. As we can see in Figs 11 – 14, the peak of the quasi-steady case lift curve is

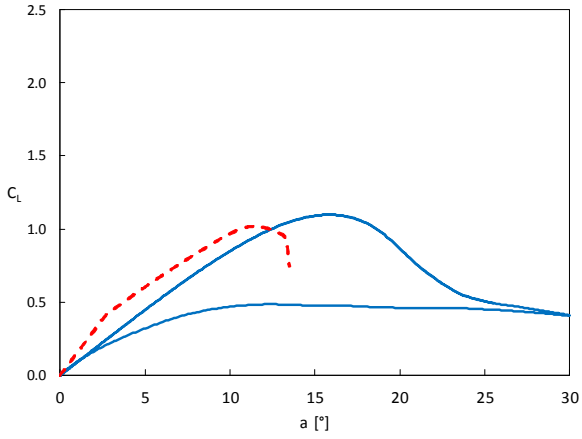

Fig. 11 Lift curve for k = 0.01 (NACA 0012, α = 0 to 30°) compared to static lift

unsteady cases the maximum steady C_L value is significantly exceeded. The steady critical angle of attack value was surpassed in all four cases. The lift curve formed different hysteresis loops for each case, as it is depicted.

For higher reduced frequencies approaching the value of 1, the lift curve becomes to be ellipse-shaped. This was also confirmed by an experimental study done by [3], during which it was observed that if the reduced frequency is increased even further, the main half-axis of the ellipse-shaped lift curve becomes almost horizontal. Ultimately, the ellipse becomes a circle.

A further reduced frequency dependency analysis was made for pitching motions of reduced frequencies of 0.05, 0.15 and 0.25, the angular range of the pitching motion being 5 to 25° and the undisturbed flow's Reynolds number being 2.5×10^6 in all cases. The differing reduced frequency affected the hysteresis loop, which appeared to shrink towards the steady lift curve as the reduced frequency increased. Also, the angle of attack corresponding to the maximum unsteady lift coefficient was greater for increased reduced frequencies – for $k = 0.05$ the lift coefficient reached its maximum at $\alpha = 22°$, whereas for $k = 0.15$ and 0.25 it was at $\alpha = 25°$.

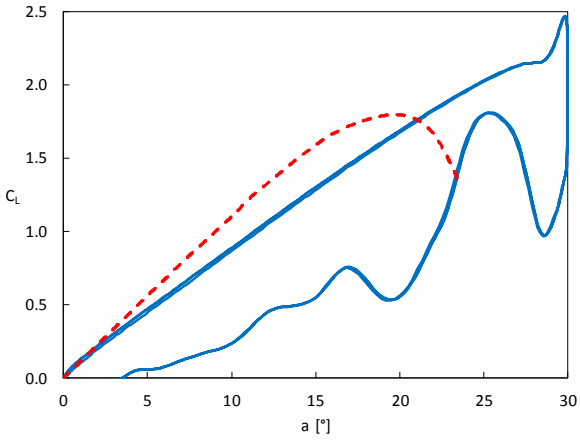

Fig. 12 Lift curve for $k = 0.12$ (NACA 0012, $\alpha = 0$ to 30°) compared to static lift

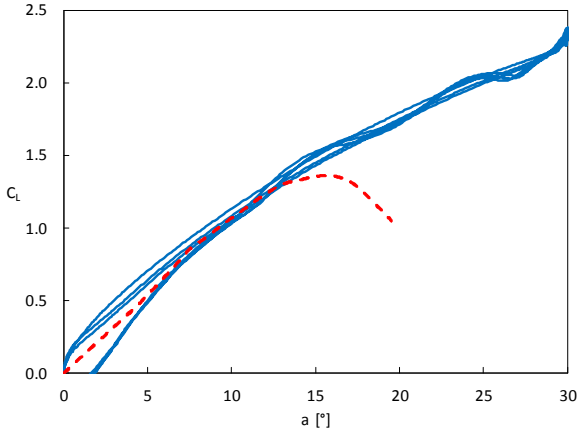

Fig. 13 Lift curve for $k = 0.47$ (NACA 0012, $\alpha = 0$ to 30°) compared to static lift

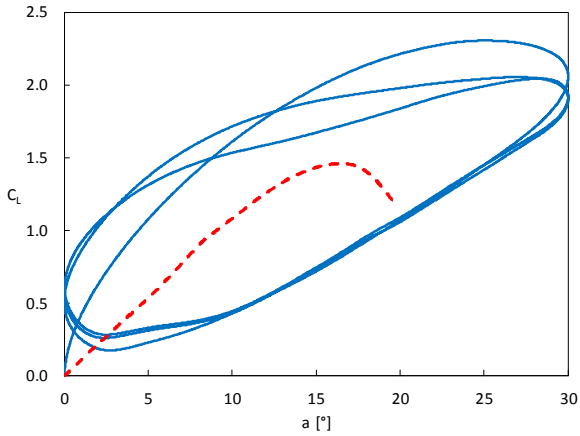

Fig. 14 Lift curve for k = 0.94 (NACA 0012, α = 0 to 30°) compared to static lift

5. Conclusion

The main goal of this paper was to study the unsteady flow over a pitching NACA 0012 airfoil to provide a detailed insight into the vortex formation and breakdown process using CFD modeling and visualization. Another goal was to compare the steady and dynamic lift coefficients of various flows, and to assess the effect of the principal flow and motion parameters on unsteady lift curves and coefficients. Nine different cases of flow were modeled, covering Reynolds numbers from 9.5×10^4 to 5.5×10^6 and reduced frequencies ranging from 0.01 to 0.94.

It can be concluded that Reynolds number does not significantly affect the lift curve, while the reduced frequency is a crucial parameter. It determines the lift curve shape, the maximum lift coefficient values, as well as corresponding angles of attack. Having done the steady versus unsteady case comparison, the maximum static coefficient of lift was exceeded by 28 to 75 %, whereas the angle of attack corresponding to the maximum lift coefficient was surpassed by 18 to 92 %, the major driving factors being the reduced frequency and the angular range of the pitching motion.

References

[1] MCALLISTER, K., CARR, L. and MCCROSKEY, W. *Dynamic Stall Experiments on the NACA 0012 Airfoil* [Technical report No. 1100]. NASA, 1978.

[2] AHMAD, K.A. et al. Numerical Modelling of a Pitching Airfoil. *Jurnal Mekanikal*, 2010, vol. 30, no. 1, p. 37-47. ISSN 2289-3873.

[3] ROZEHNAL, D. and SVOBODA, A. *Unsteady Measurement of Aerodynamic Characteristics of a Profile During Dynamic Stall* [Internal Report]. Brno: University of Defence, K-204/A, 2008.

[4] LOWSON, M. Some Experiments with Vortex Breakdown. *The Aeronautical Journal*, 1964, vol. 68, no. 641, p. 343-346. ISSN 0001-9240.

[5] KRISHNAMOORTHY, V. *Vortex Breakdown and Measurements of Pressure Fluctuations over Slender Wings* [Ph.D. thesis]. The University of Southampton, 1966.

[6] WOODGATE, L. *Measurements of the Oscillatory Pitching-Moment Derivatives on a Sharp-Edged Delta Wing at Angles of Incidence for Which Vortex Breakdown Occurs.* Aeronautical Research Council, R.&M. 3628, Part III, 1971.

[7] WOLFFELT, K. *Investigation on the Movement of Vortex Burst Position with Dynamically Changing Angle of Attack for a Schematic Delta Wing in a Water Tunnel with Correlation to Similar Studies in Wind Tunnel, Aerodynamic and Related Hydrodynamic Studies Using Water Facilities*. AGARD-CP-413, 1987.

[8] ATTA, R. and ROCKWELL, D. Hysteresis of Vortex Development and Breakdown on an Oscillating Delta Wing. *AIAA Journal*, 1987, vol. 25, no. 11, p. 1512-1513. ISSN 0001-1452.

[9] ATTA, R. and ROCKWELL, D. Leading-edge Vortices due to Low Reynolds Number Flow Past a Pitching Delta Wing. *AIAA Journal*, 1990, vol. 28, no. 6, p. 995-1004. ISSN 0001-1452.